

# EVLA Memo 157

## Further investigation of low-level correlator artifacts: Wobbles and splatter

R.J. Sault

25 March 2011

### Introduction

WIDAR is the powerful and sophisticated back-end to the EVLA system. A requirement for WIDAR has been a flexibility to support a diverse set of EVLA science over coming decades. Ultimately power, sophistication and flexibility lead to complexity and a large parameter space of ways to configure the correlator. Pitfalls can be lurking in this large, dark, space. This memo presents an analysis of a family of WIDAR artifacts that have become known as “wobble” and “splatter”. Wobble is an oscillation in baseline amplitude and phase of continuum observations. The oscillations are up to about  $10^\circ$  in phase of several percent in amplitude. Splatter are artifacts in the spectra of line observations where emission is scattered from one channel to another at the level of several parts in  $10^2$  or smaller. Both wobble and splatter are non-closing effects. These effects are shown to have an origin in some finite precision aspects in the individual WIDAR lag cells. Specifically they result from the finite precision of the phase model and the three-level nature of the phase rotator. Wobble/splatter would not result if either the phase model or the phase rotator were perfect: they result only through an interaction between the two. Work-arounds to avoid these artifacts are readily implementable.

The MERLIN correlator, which uses a similar design, may also be susceptible to these effects.

This memo builds on the work of a plethora of WIDAR memos (in particular NRC-EVLA memos 32, 24 and 1) and NRAO EVLA memo 148.

This memo addresses “classic” splatter which is the predominant issue seen in EVLA memo 148. NRC-EVLA memo 32 considers this “classic” splatter, but does not offer a mechanism. However the memo notes another splatter-like phenomenon which is caused by a beating between the so-called  $f_{\text{shift}}$  frequencies of antennas and the dump rate of the correlator chip. The latter effect is smaller than “classic” splatter by a factor of  $\sim 20$ . It is well described in NRC-EVLA memo 32 and will not be considered here further.

### WIDAR lag cell architecture

At its simplest, the signal from each EVLA antenna is filtered, downconverted, sampled, digitally filtered and then routed to an array of lag cells. The lag cells perform the correlation between the two antenna signals. In the digital filtering stage, multiple sub-bands can be formed. A visibility spectrum for a sub-band for each pair of antennas is formed by Fourier transforming the lags for those antennas.

A novel characteristic of the design of WIDAR is the so-called “phase washing” (also called “fringe washing”) technique. Phase washing provides anti-aliasing suppression between adjacent sub-bands which is in addition to the digital filter bandpass response. Phase washing helps beat down a number of other systematic effects, such as sampler offsets.

The phase washing technique introduces an antenna-specific frequency offset,  $f_{\text{shift}}$ , in the LO at the downconversion stage. Depending on the bandwidth being used, this offset is typically hundreds of Hertz to hundreds of

kilohertz. This frequency offset is removed by the phase rotator in the lag cell. The phase washing technique is closely related to the decorrelating effect that the natural astronomical fringe rate has on some undesired signals. Phase washing also has commonality with the traditional approach of Walsh switching used in many interferometers.

Figure 1 gives a block diagram of a WIDAR lag cell. It has a multiplier to correlate the two real-valued antenna signals. This multiplier output will have a winding phase. This phase rate is stopped by a complex-valued phase rotator (mixer). The output of the phase rotator can then be accumulated in a complex-valued store. The phase for the phase rotator comes from a phase model stream that accompanies each antenna data stream. For the purposes needed here, the winding phase at the multiplier output (and the phase model which is intended to represent this) is the sum of:

- the fringe phase of that antenna relative to some reference point (for the EVLA, the fringe phase is computed relative to the center of the wye), and
- the phase resulting from the  $f_{\text{shift}}$  frequency introduced into each antenna.

Alternatively we can say the frequencies of the phase model rates for antennas 1 and 2 are the sum of the fringe rates and the  $f_{\text{shift}}$  frequencies:

$$\begin{aligned}\nu_1 &= \nu_{\text{fringe},1} + \nu_{\text{shift},1}, \\ \nu_2 &= \nu_{\text{fringe},2} + \nu_{\text{shift},2}.\end{aligned}$$

The phase applied by the phase rotator is thus  $2\pi(\nu_1 - \nu_2)t$ . Applying this phase stops the phase-winding in the multiplier output and allows the result to be usefully integrated.

If either the phase rotator or the phase models were perfect, there would be no wobble/splatter. However the phase rotator and phase models both are implemented with limited precision.

In the WIDAR design, the phase rotator is a three-level one - see Figure 2. This rotator generates odd harmonics in addition to the fundamental. The harmonic coefficient (i.e. the amplitude) of the 3rd, 5th and 7th harmonics are of order 25% of the fundamental. These harmonics will introduce an error in the output. If we assume ideal phase models, then for visibility,  $V$ , integration time  $T$  and harmonic  $n$ , and harmonic coefficient  $a_n$  ( $\sim 0.25$ ) then the error in output will be

$$a_n V \text{sinc}\left((n-1)(\nu_1 - \nu_2)T\right).$$

As the  $f_{\text{shift}}$  frequencies are chosen to ensure  $\nu_1 - \nu_2$  is appreciable, this error dies away rapidly, and can be ignored. Rather simply, for an ideal phase model, the odd harmonics of the phase rotator do not correlate with anything - they do not phase stop the astronomical signal.

Unfortunately the phase models are not ideal. Although the phase model for a sample is computed with high precision in the antenna-based processing of WIDAR, it is quantized to 4 bits (i.e.  $22.5^\circ$  resolution) when distributed with the antenna data streams<sup>1</sup>. If the phase models were carried with infinite precision, the phase rotator would transition between +1 to 0, or 0 to -1 cleanly. A consequence of the quantization is that there is a form of phase noise in the phase model and their differences. This phase noise introduces extra harmonics. An example of this is that, rather than transitioning cleanly, the phase rotator can dither at the transition boundary. A simple instance is shown in Figure 3. Phase quantization and dither introduces additional harmonics. In particular the phase rotator will produce odd harmonics of the frequencies  $\nu_1$  and  $\nu_2$ , and their sums and differences - not just the odd harmonics of the difference frequency  $\nu_1 - \nu_2$ . A convenient representation of the harmonic frequencies generated by the phase rotator is

$$\nu = (\nu_1 - \nu_2) + 2m\nu_1 - 2n\nu_2$$

where  $m$  and  $n$  are (positive and negative) integers. The values  $(m, n) = (0, 0)$  corresponds to the fundamental and  $(m, n) = (1, 1)$  corresponds to the third harmonic of  $\nu_1 - \nu_2$ .

---

<sup>1</sup>The phase model is quantized by truncation rather than rounding. Although truncation is normally thought of as a source of systematic offsets, it has no affect here. This is because phase is a cyclic quantity and because it is the difference with another truncated phase which is important.

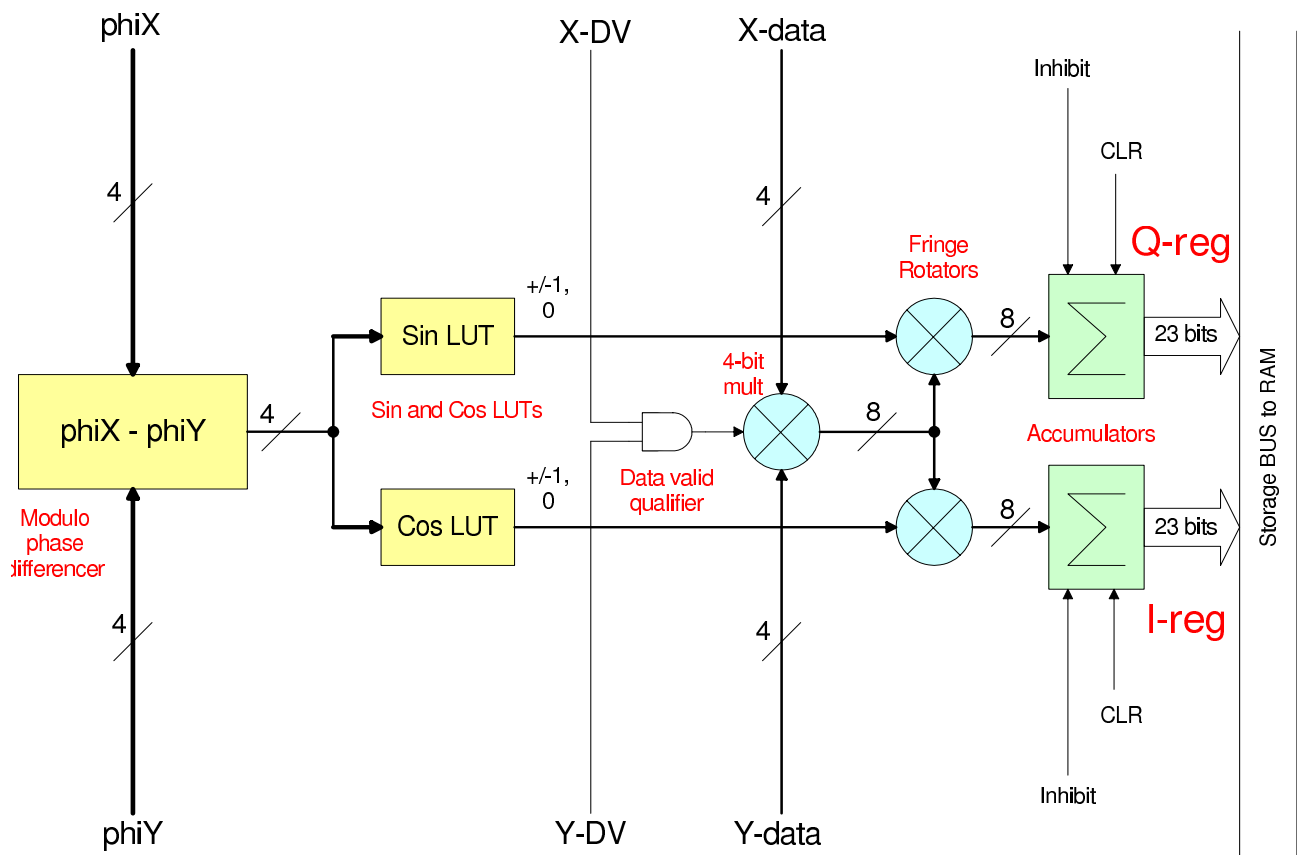


Figure 1: WIDAR lag cell. The antenna data, X-data and Y-data are multiplied and the result fed to a phase rotator. The input to the phase rotator are the phase models,  $\phi_X$  and  $\phi_Y$ , which are differenced. This difference is fed to sine and cosine lookup tables (LUTs) and two 3-level multipliers (“Fringe Rotators” in the diagram).

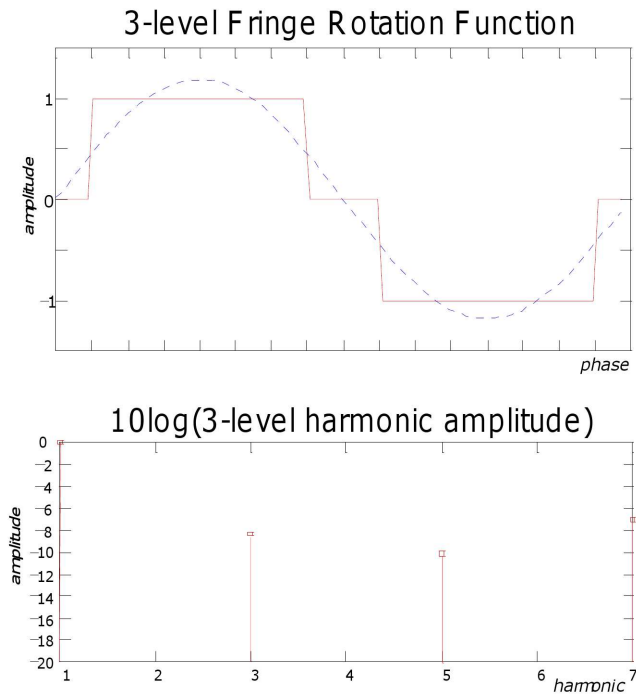


Figure 2: Three-level phase rotator response and the harmonics generated.

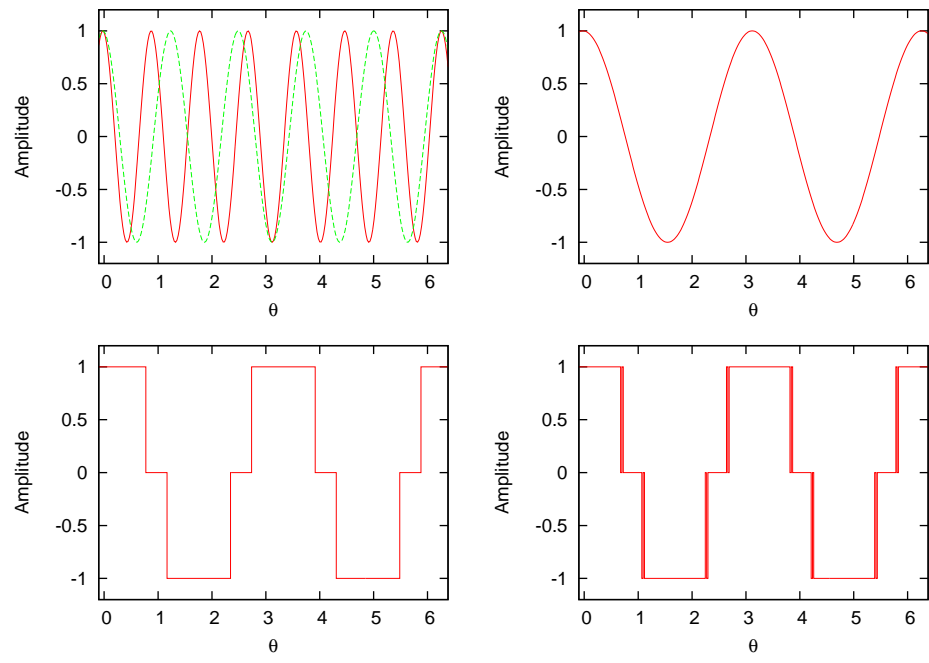


Figure 3: Representations of cosinusoids. Top left shows two cosinusoids,  $\cos(\omega_1 t)$  and  $\cos(\omega_2 t)$ . Top right is  $\cos((\omega_1 - \omega_2)t)$ . Lower left is the three-level representation of this function where the phases are differenced at full precision. In the lower right, the phases are rounded to 4 bits before differencing. The dither near transitions is apparent. Dithering is a function of the relative phase of the two the signals.

## Wobble and splatter

The wobble and splatter effects come about when there are harmonics (i.e. in addition to the fundamental) that phase stop the astronomical signal. The condition for this is  $m\nu_1 \sim n\nu_2$ , or more formally when

$$|m\nu_1 - n\nu_2|T < 1.$$

This will cause an additional component in the output visibility. Small values of  $m$  and  $n$  will generally cause more significant errors both because the harmonic coefficients for small  $m$  and  $n$  are larger and because components with larger  $m$  and  $n$  smear out more rapidly with integration time  $T$ .

Although one can think of a forest of harmonics for all values of  $m$  and  $n$ , in practice it is only necessary to consider the instances where  $m$  and  $n$  are mutually prime. For example the harmonics  $(m, n) = (1, 3), (2, 6), (3, 9), \dots$  are all in the ratio 1:3 and will all affect the same correlation. It is the sum of the effects of these harmonics that will be seen in the astronomical data.

For continuum observations, the wobble phenomena is a modulation of the visibility data. The wobble frequency seen on a baseline will depend be the residual rate,  $m\nu_1 - n\nu_2$ , multiplied by a small integer. This small integer,  $r$ , is a function of  $m$  and  $n$ . Although  $r$  will be the same for real and imaginary parts, it can be different for the correlation amplitude and phase. As the residual rate becomes more significant and comparable with the integration dump rate, the wobble oscillation will be modulated further by a sinc function.

For spectral line experiments, the wobble effect is seen in the *lag domain*. When this wobbly lag spectrum is Fourier transformed to the visibility domain, the lag wobble turns into a spectral “splatter”. Exactly the same wobble patterns can seen in the lag domain of a spectral observation as wobbles patterns in the time domain of a continuum observation. Most of the remaining discussion will focus on wobble. In general a corresponding statement could be made about splatter.

Assuming they use the same  $f_{\text{shift}}$  frequencies, wobble/splatter will affect both polarizations equally. However there is no requirement for the wobble patterns of the two polarizations to be in phase. Small differences in the phase model between polarizations (e.g. different instrumental delays resulting in different fractional delay corrections) will cause significant changes in the wobble phase.

## Guidelines for avoiding wobble and splatter

Under what circumstances with the phase rates on two antennas be related by small integers? Recall that

$$\begin{aligned}\nu_1 &= \nu_{\text{fringe},1} + \nu_{\text{shift},1}, \\ \nu_2 &= \nu_{\text{fringe},2} + \nu_{\text{shift},2},\end{aligned}$$

where the fringe frequencies are those of the antenna relative to the reference point (i.e. normally relative to the center of the wye).

Current practice at the EVLA is to set the  $f_{\text{shift}}$  frequencies to a value that is generally much larger than the fringe frequencies. So in practice there is a potential for wobble on a baseline only if the  $f_{\text{shift}}$  frequencies on two antennas are related by small integers. For those antennas, wobble will occur when the fringe rates for those antennas are (nearly) related by the same small integers. Clearly allowing the  $f_{\text{shift}}$  frequencies to be related by small integers should be avoided. In practice this step alone should eliminate the wobble/splatter issue. It has recently become standard at the EVLA for  $f_{\text{shift}}$  frequencies to be chosen so that this requirement is *usually* met.

The current EVLA system requires that the  $f_{\text{shift}}$  frequencies are multiples of 100 Hz. In addition, the maximum  $f_{\text{shift}}$  frequency should not generally be larger than a small fraction of the sub-band bandwidth. For narrow bandwidth observations, these two constraints leave little flexibility in the choice of  $f_{\text{shift}}$  frequencies. For example, for bandwidths of 500 kHz and narrower, there is no flexibility to avoid  $f_{\text{shift}}$  frequencies that are related by small integers. In this case, wobble/splatter will occur when the fringe frequency of the antennas (relative to the reference point) are related by the same integers as the  $f_{\text{shift}}$  frequencies. In the course of a long observation, it will be common for a source to transit through a region where the fringe frequencies are related

by the same integers. This was a common experience with the wobble phenomenon: a baseline will be seen to go ‘bad’ for a period and then come good again.

The wye geometry of the EVLA and the use of the wye center as reference presents some special cases. Because the baseline lengths along an arm are not related by integers, the fringe frequencies of antennas along an arm are generally not related by small integers. The exception is when the source azimuth aligns with the arm: at this time the fringe frequency is 0 for all the antennas and the fringe rates do not help in eliminating the problem. So for the baselines within an arm, wobble/splatter will generally not occur *regardless* of the ratios of the  $f_{\text{shift}}$  frequencies. The exception to this is when the source azimuth aligns with the arm, and then wobble/splatter will be seen on *all* baselines where the  $f_{\text{shift}}$  frequencies are related by small integers.

For observations with narrow sub-bands, where small integer relationships between antenna  $f_{\text{shift}}$  frequencies cannot be avoided, it would be possible to move the reference point for fringe frequency calculation to somewhere other than the center of the wye. Appropriate selection will likely reduce the area of the sky where wobble/splatter is problematic. Such a reference point would not be on the line of an arm and be distant enough so that the fringe frequencies are comparable in magnitude to the  $f_{\text{shift}}$  frequencies.

Assuming that the  $f_{\text{shift}}$  frequencies and the fringe rates are both related by the same integers, then if wobble is seen at a high frequency it will also be present at lower frequencies (all else being equal). The wobble frequency will scale with observing frequency. The converse is not true: the presence of a wobble at low observing does not require a wobble to be seen at higher observing frequency. It is possible for  $|m\nu_1 - n\nu_2|T$  to be small at low frequencies but large at high frequencies.

Wobbles will be more common when fringe rates are low. In particular wobbles will be more common at low frequencies, in more compact arrays and sources at higher declination.

## Some examples

The wobble/splatter effect is relatively easy to simulate and to compare with observed data. The simulation can reproduce the size of phase wobbles (in degrees) and the relative size of amplitude wobbles. The starting point in the wobble pattern is dependent on instrumental parameters that are not generally accessible, and so in the examples that follow the starting point of the wobble pattern has been adjusted to match the observed wobble pattern.

Figure 4 shows observed and simulated wobbles for a continuum observation between VLA stations W01 and N05 for an observing frequency of 9 GHz. The  $f_{\text{shift}}$  frequencies were in the ratio of 1:5. Both amplitude and phase wobbles are prominent for this set-up. The panels on the left show the observed wobbles, whereas those on the right give predicted wobbles. Note that when the wobble pattern period is comparable to the correlator dump time, there will be some reduction in the amplitude of the wobble pattern caused by smearing. The simulation software does no account for this. In the example of Fig. 4, the phase wobble will experience some modest smearing, which is the cause for the peak-to-peak size of the observed phase wobble being somewhat smaller than the prediction.

Figure 5 shows a lag spectrum for an actual and a simulated CW tone observation. The observation was set to phase and delay track the north celestial pole, whereas the antennas were physically stowed. The CW tone made it into the feedhorns via primary beam sidelobes. The  $f_{\text{shift}}$  frequencies were in the ratio of m:n=1:3. The match between simple simulation software and the observation is very good.

## Appendix A: Fringe frequencies

The fringe frequency of an antenna is proportional to the length of the projection onto the Earth’s equatorial plane of the displacement vector from the reference point to the antenna. Ignoring the change in the annual component over a day (which is small here), the fringe frequency varies sinusoidally with a period of a sidereal day. The zero crossings depend on the displacement vector geometry (e.g. for an east-west displacement vector, the fringe frequency is 0 at source hour angles of 0 and 12 hours; for a north-south vector, it is zero at  $\pm 6$  hours). In general, for arbitrary real values  $a$  and  $b$ , there will always be two times during a sidereal day when

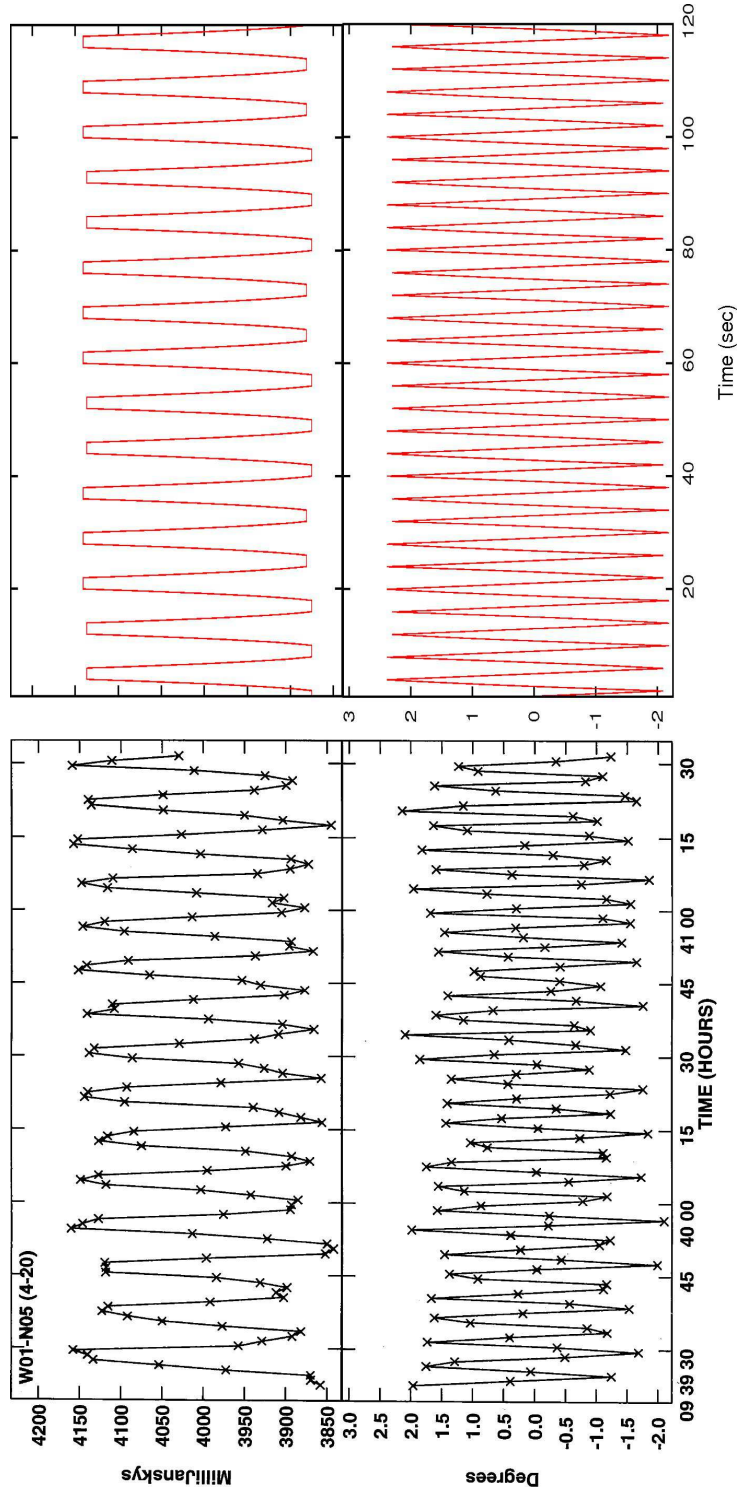


Figure 4: Observed (left panels) and simulated (right panels) wobble patterns in both amplitude (upper panels) and phase (lower panels). This is for a continuum observation at 9 GHz where the  $f_{\text{shift}}$  frequencies were in the ratio of  $m:n=1:5$ . The visibility amplitude plots are in mJy, whereas the visibility phase plots are in degrees.

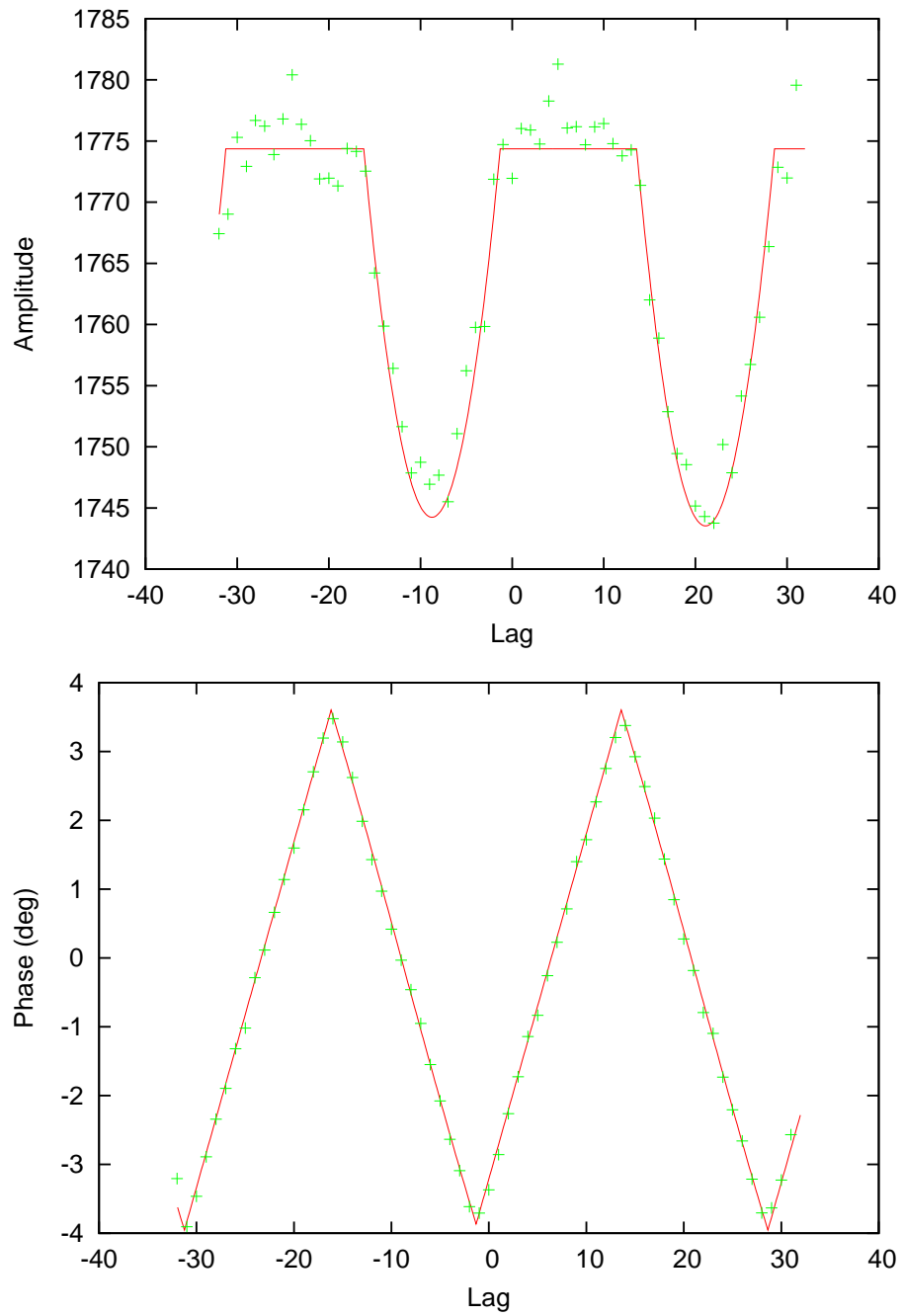


Figure 5: Splatter,  $m:n=1:3$ . The plus symbols are the observed data, whereas the lines are simulations of the pattern.

the scaled fringe frequencies for two antennas  $a\nu_{\text{fringe},1}$  and  $b\nu_{\text{fringe},2}$  will be equal. That is, there are two points where the fringe frequency sinusoids cross each other.

When the two antennas and the reference point are all co-linear (e.g. the case the antennas in the same arm of the EVLA when the wye center is used as the reference), then the antenna fringe rates will have the same zero crossing points. Because the spacing from the wye center to different antennas are not related by simple integers, there are no cases where  $m\nu_{\text{fringe},1} = n\nu_{\text{fringe},2}$  (for integers  $m$  and  $n$ ). So the only cases where integer-scaled fringe frequencies on an arm are equal are at the zero crossings.